Electronic Supplementary Material (ESI) for Nanoscale.

Supplementary Information

Clinical big-data-based design of GLUT2-targeted carbon nanodots for the accurate diagnosis of hepatocellular carcinoma

Hye Jin Heo[1,§], Yoonsang Park[2,3,§], Jung Hee Lee[4,§], Yujin Kim[5], Eun Kyoung Kim[1], Ga Hyun Kim[6], Yeoni Yu[7], So Youn Park[8], Hie Bum Seo[9], Kyoungjune Pak[7,10], Tae Sik Goh[7,11], Sae-Ock Oh[1,], Woosung Kwon[2,5,*], Yun Hak Kim[1,7,12,*]*

[1]Department of Anatomy, School of Medicine, Pusan National University, Yangsan 50612, Republic of Korea

[2]Institute of Advanced Materials and Systems, Sookmyung Women's University, Seoul 04310, Republic of Korea

[3]Nano Convergence Technology Research Center, Korea Electronics Technology Institute (KETI), Seongnam 13509, Republic of Korea

[4]Department of Pathology, School of Medicine, Pusan National University, Yangsan 50612, Republic of Korea

[5]Department of Chemical and Biological Engineering, Sookmyung Women's University, Seoul 04310, Republic of Korea

[6]Interdisciplinary Program of Genomic Data Science, Pusan National University, Yangsan 50612, Republic of Korea

[7]Biomedical Research Institute, Pusan National University Hospital, Yangsan 50612, Republic of Korea

[8]Gene & Cell Therapy Research Center for Vessel-associated Diseases, Pusan National University, Yangsan 50612, Republic of Korea

[9]Department of Radiology, School of Medicine, Pusan National University, Pusan National University Hospital, Yangsan 50612, Republic of Korea

[10]Department of Nuclear Medicine, Pusan National University Hospital, Yangsan 50612, Republic of Korea

[11]Department of Orthopaedic Surgery, Pusan National University Hospital, Yangsan 50612, Republic of Korea

[12]Department of Biomedical Informatics, School of Medicine, Pusan National University, Yangsan 50612, Republic of Korea

[§]These authors equally contributed to this work.

*Corresponding author.

Tel: +81-51-510-8045; Fax: +82-51-510-8049; E-mail: hedgehog@pusan.ac.kr

Tel: +82-2-2077-7398; Fax: +82-2-2077-7450; E-mail: wkwon@sookmyung.ac.kr

Tel: +82-51-510-8091; Fax: +82-51-510-8049; E-mail: yunhak10510@pusan.ac.kr

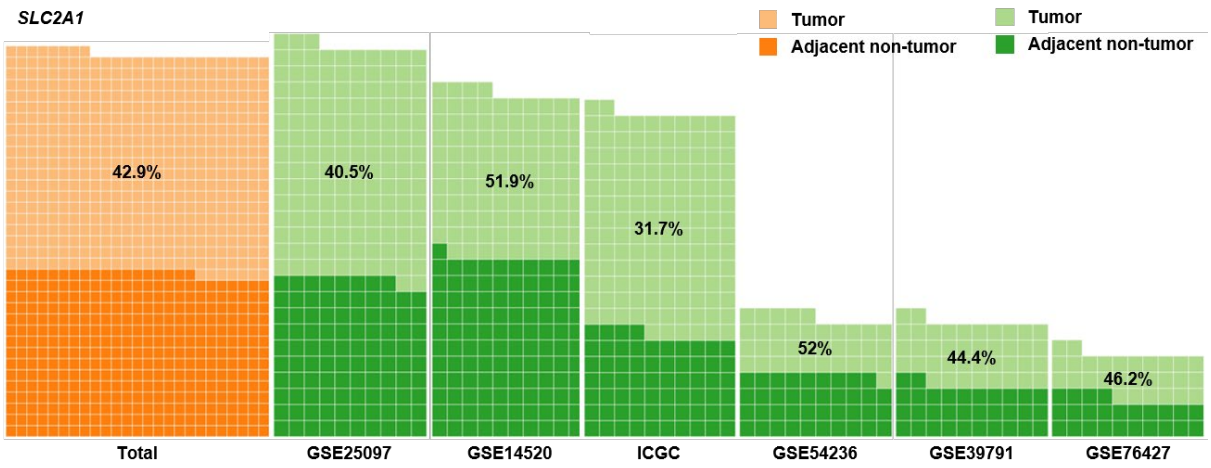

Figure S1. Differences in *SLC2A1* expression between tumor and adjacent non-tumor tissues.

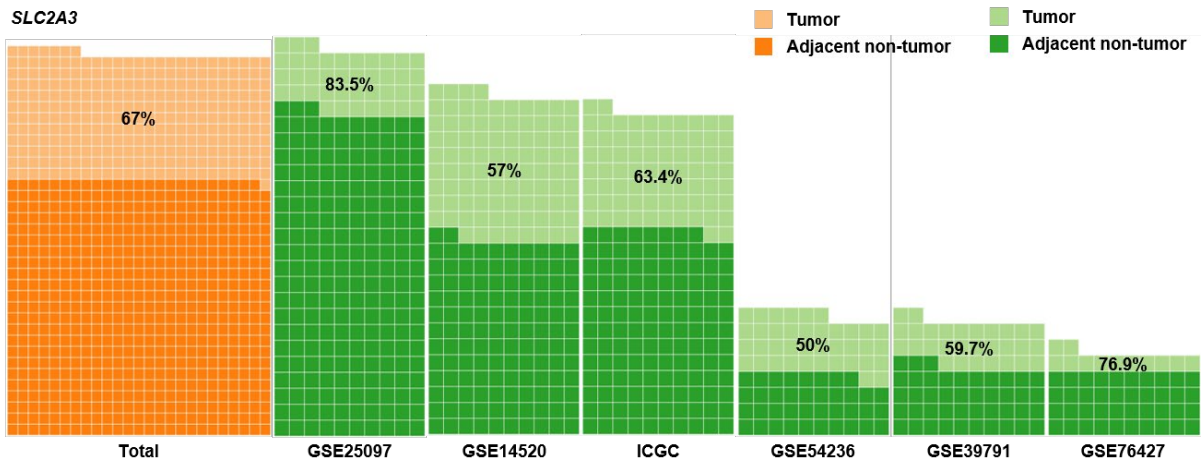

Figure S2. Differences in *SLC2A3* expression between tumor and adjacent non-tumor tissues.

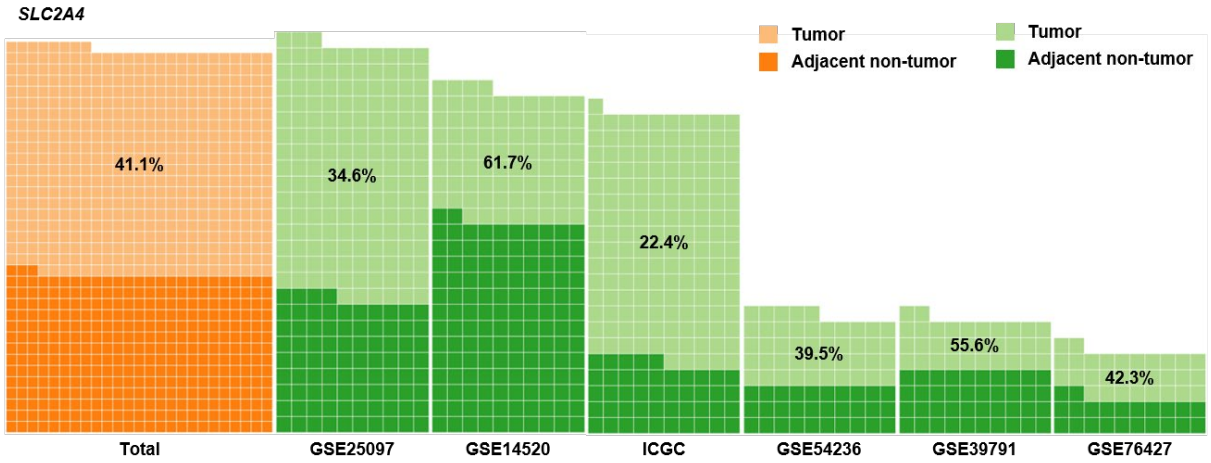

Figure S3. Differences in *SLC2A4* expression between tumor and adjacent non-tumor tissues.

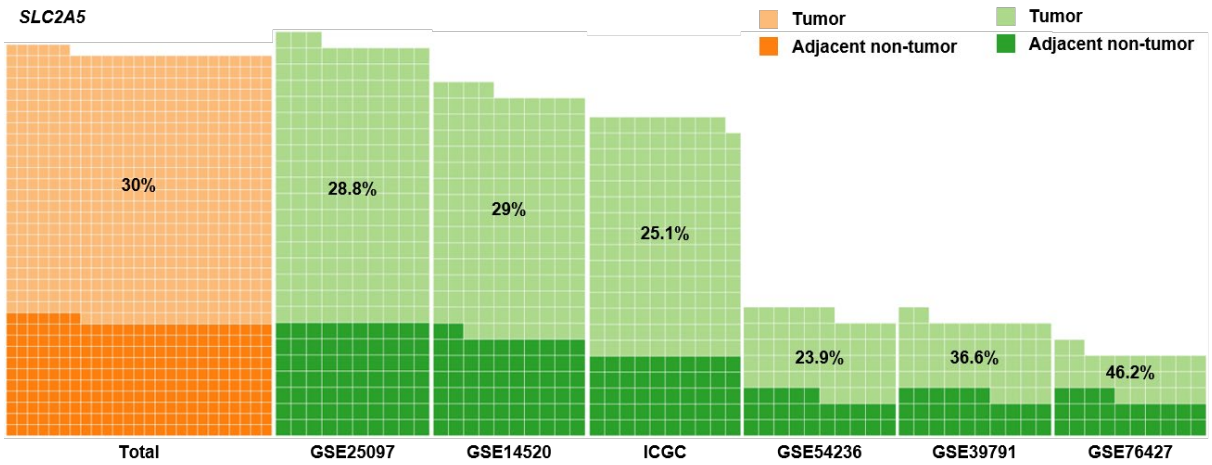

Figure S4. Differences in *SLC2A5* expression between tumor and adjacent non-tumor tissues.

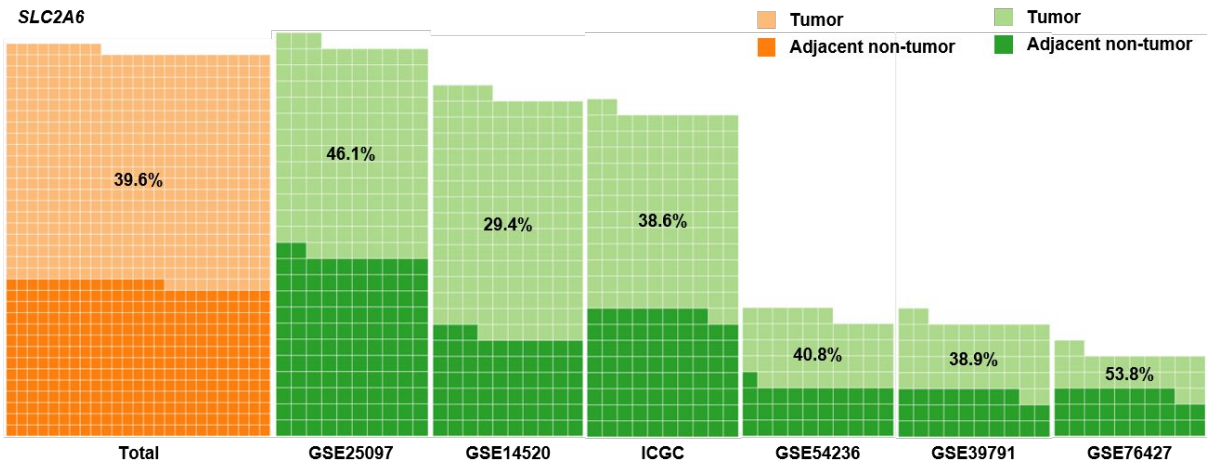

Figure S5. Differences in *SLC2A6* expression between tumor and adjacent non-tumor tissues.

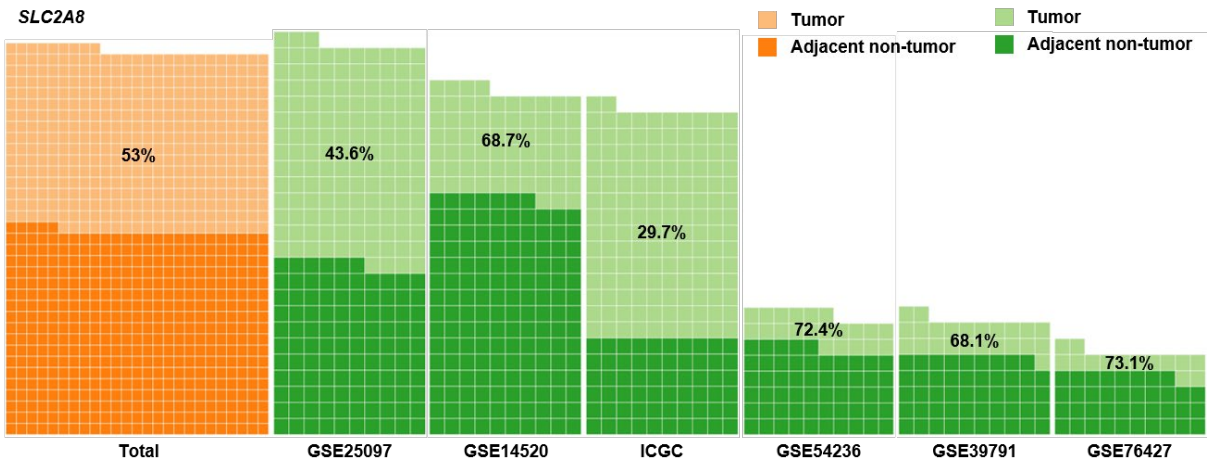

Figure S6. Differences in *SLC2A8* expression between tumor and adjacent non-tumor tissues.

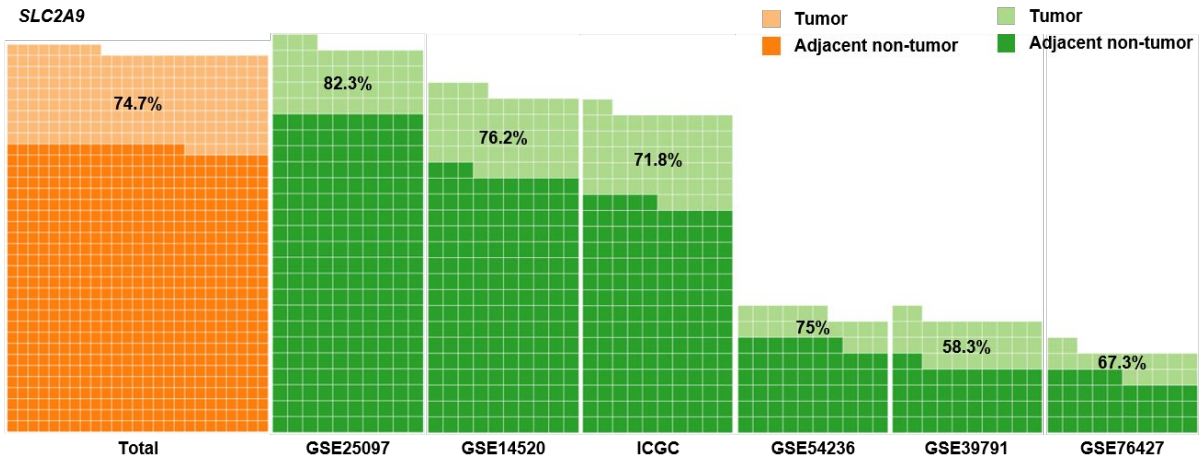

Figure S7. Differences in *SLC2A9* expression between tumor and adjacent non-tumor tissues.

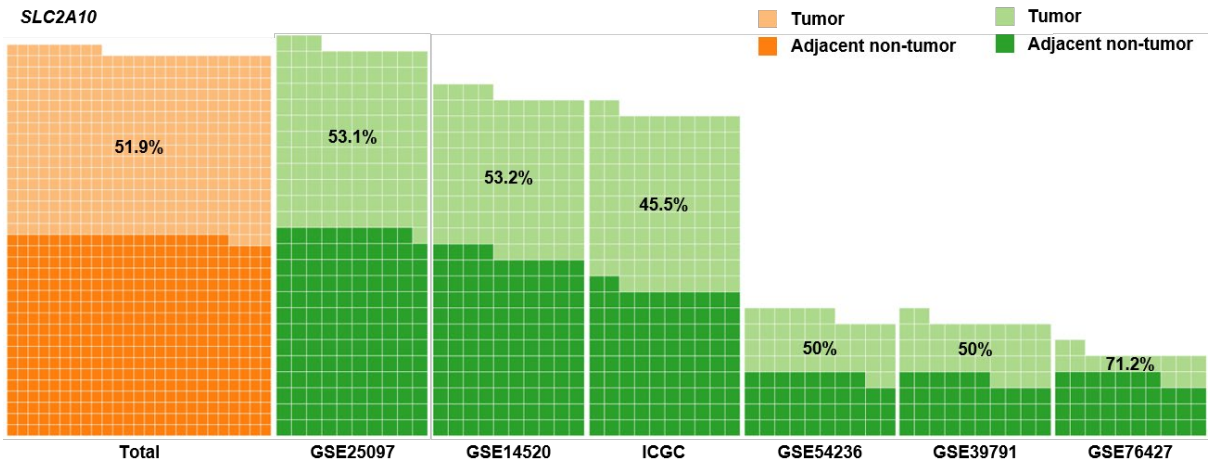

Figure S8. Differences in *SLC2A10* expression between tumor and adjacent non-tumor tissues.

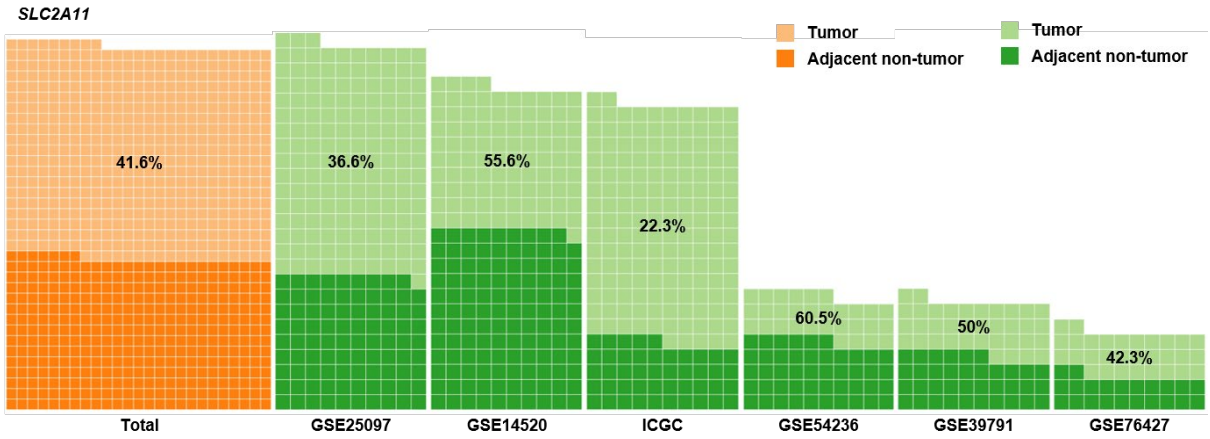

Figure S9. Differences in *SLC2A11* expression between tumor and adjacent non-tumor tissues.

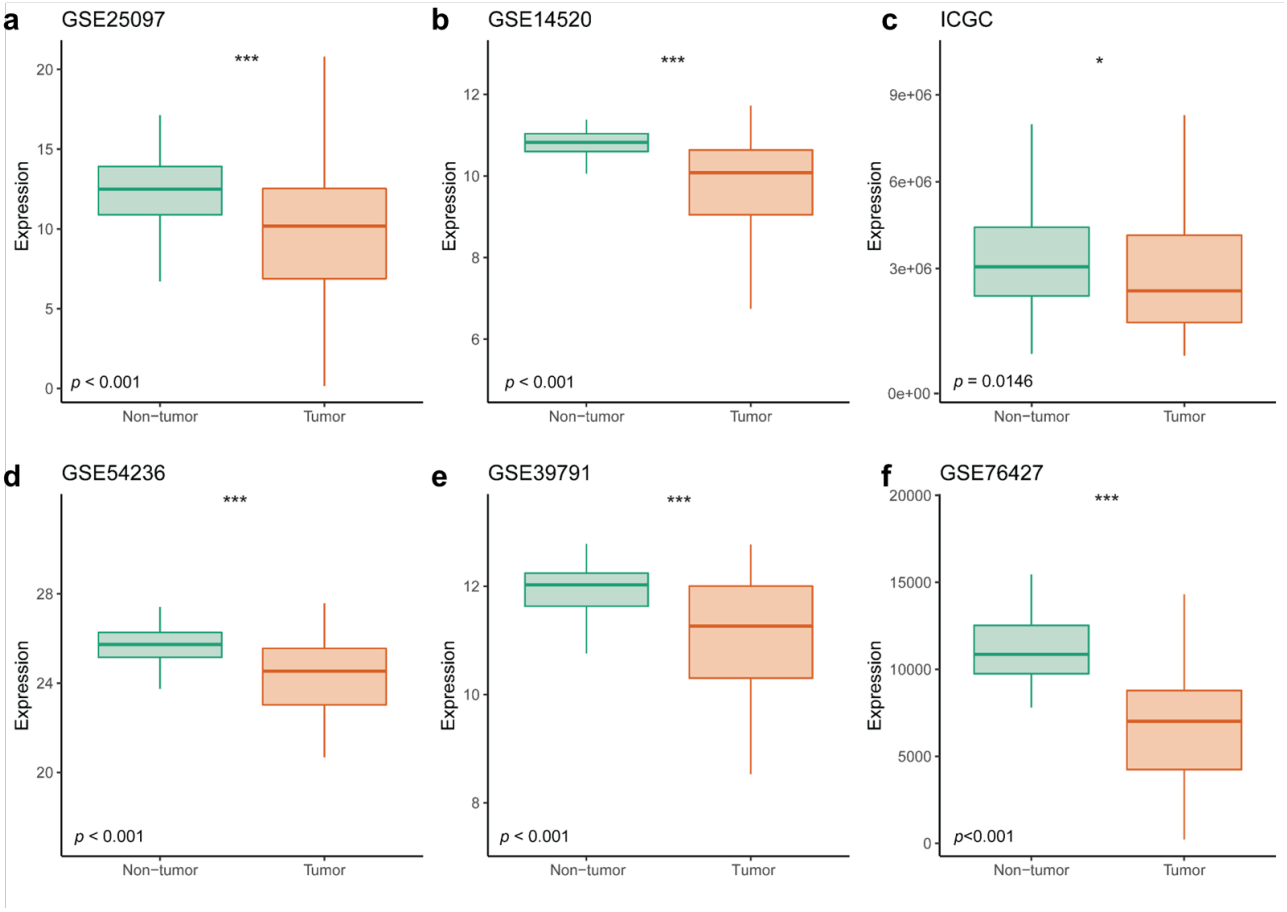

Figure S10. Boxplots of *SLC2A2* expression between tumor and adjacent non-tumor tissues in (a) GSE25097, (b) GSE14520, (c) ICGC, (d) GSE54236, (e) GSE39791, and (f) GSE76427.

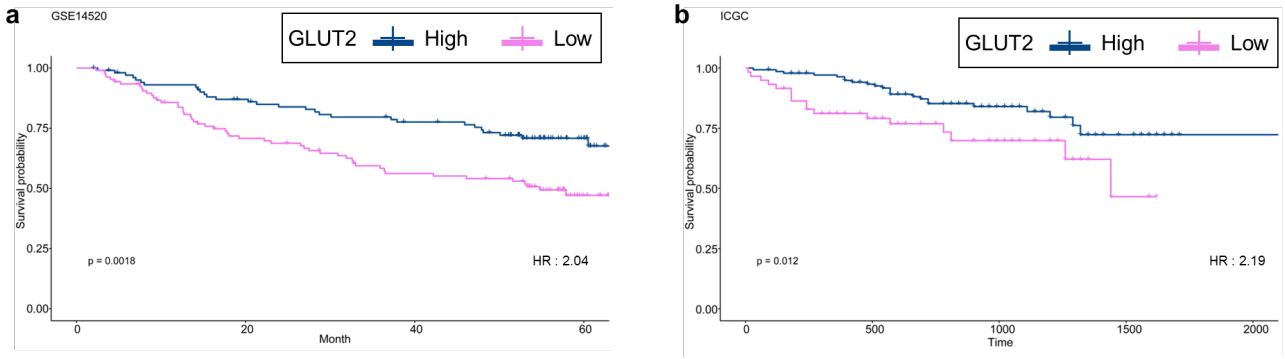

Figure S11. Kaplan-Meier estimates of HCC patient survival according to SLC2A2 gene expression from (a) GSE14520, and (b) ICGC.

Table S1. The relationship between GLUT2 intensity from immunohistochemical stain and tumor size (The HCC and adjacent normal tissues obtained from the Pusan National University Hospital, IRB No. H-1609-002-001).

GLUT2 intensity (tumor)	Tumor size				Total	P value (Fisher's exact test)
	~ 1.9cm	2cm ~ 4.9cm	5cm ~ 6.9cm	7cm ~		
1	10 (11.6%)	59 (68.6%)	6 (7.0%)	11 (12.8%)	86	0.081
2	13 (15.7%)	58 (69.9%)	9 (10.8%)	3 (3.6%)	83	
3	8 (28.6%)	15 (53.6%)	4 (14.2%)	1 (3.6%)	28	

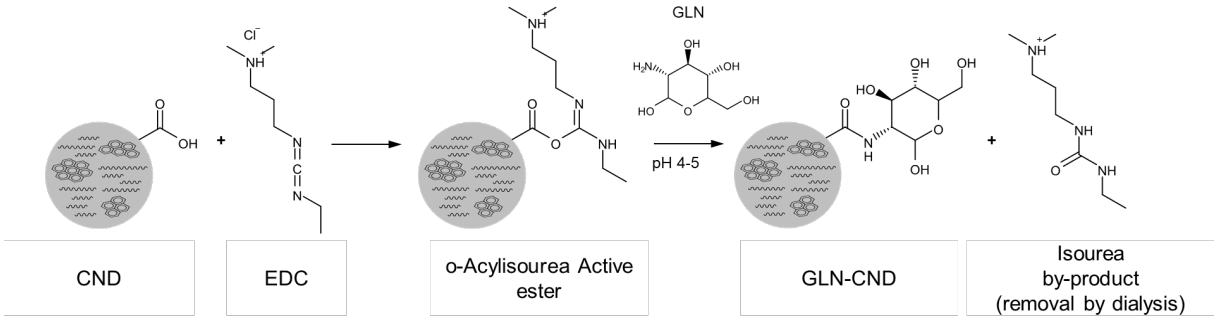

Figure S12. Chemical crosslinking mechanism between CND and GLN.

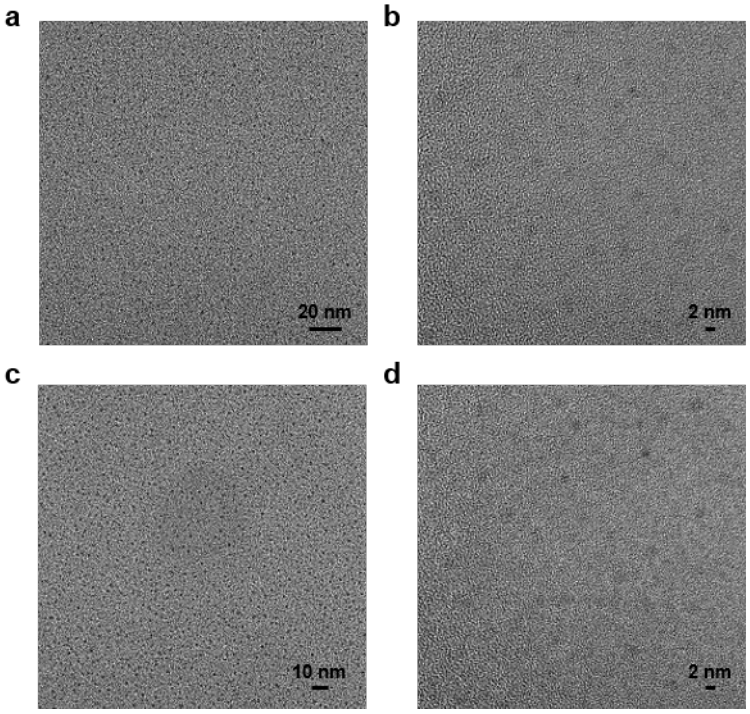

Figure S13. Additional TEM images of (A, B) CNDs and (C, D) GLN-CNDs.

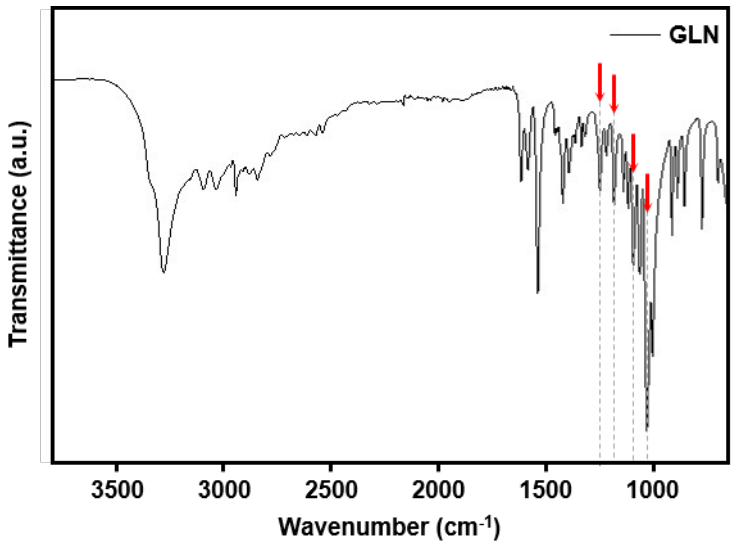

Figure S14. The IR spectrum of GLN. Red arrows indicate the characteristic signals of GLN molecules observed in the IR spectrum of GLN-CNDs.

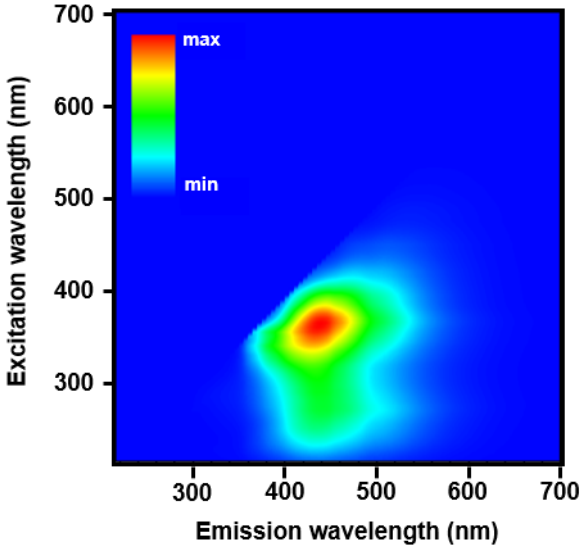

Figure S15. Photoluminescence emission map of CNDs.

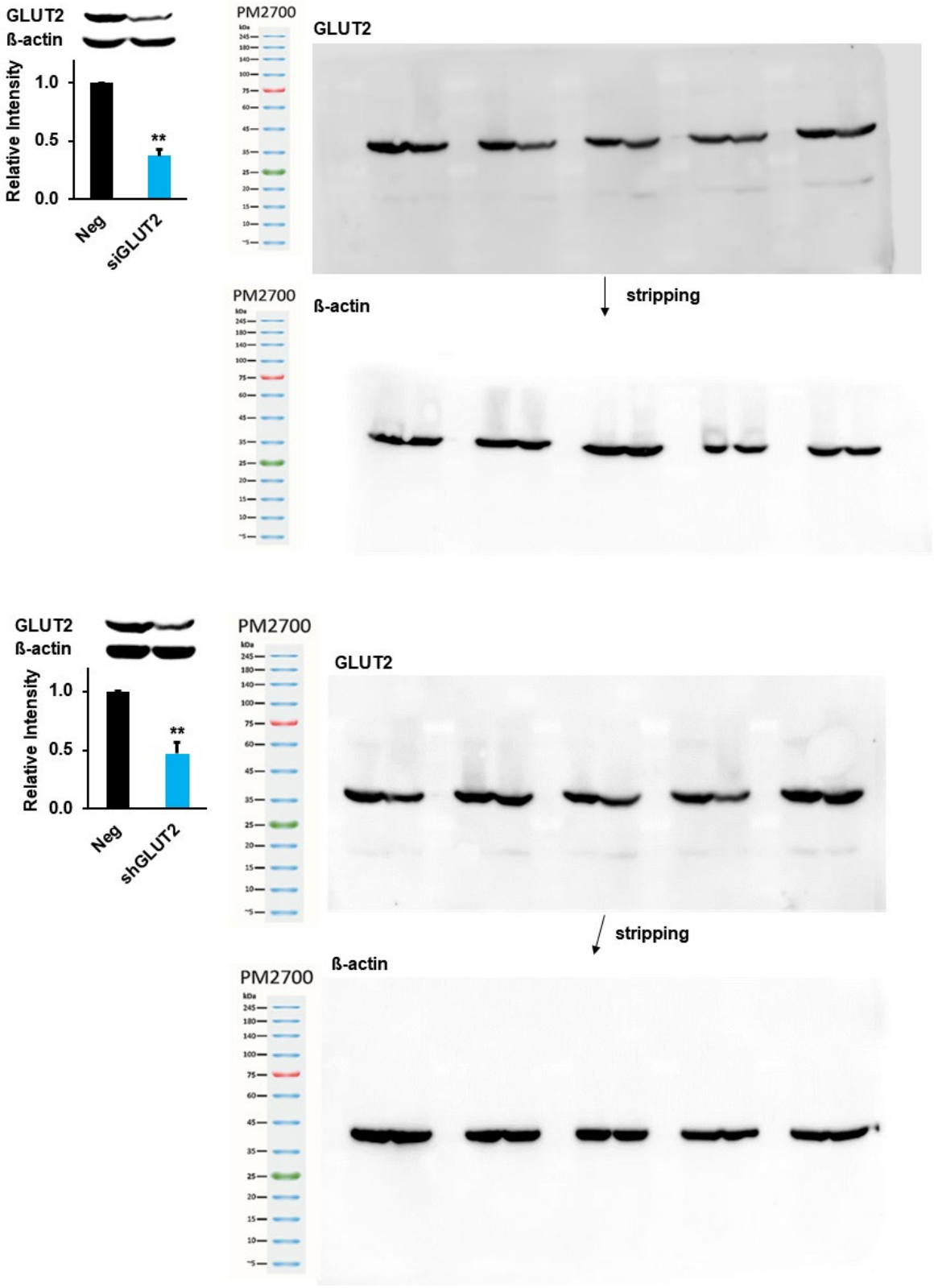

Figure S16. Raw Western blot data provided as per the journal data policy.

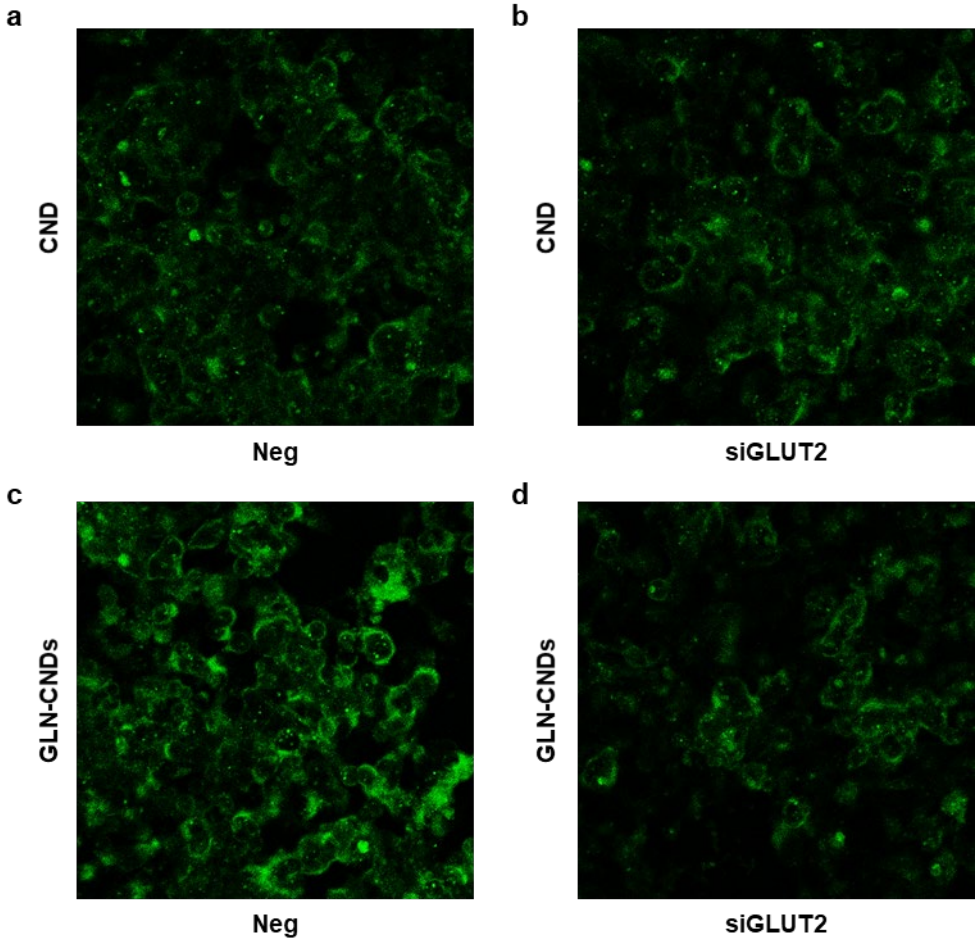

Figure S17. Comparison of binding affinity of CND and GLN-CNDs based on GLUT2 expression. Cells were stained with (A, B) CND and (C, D) GLN-CNDs. Images were obtained by confocal microscopy.

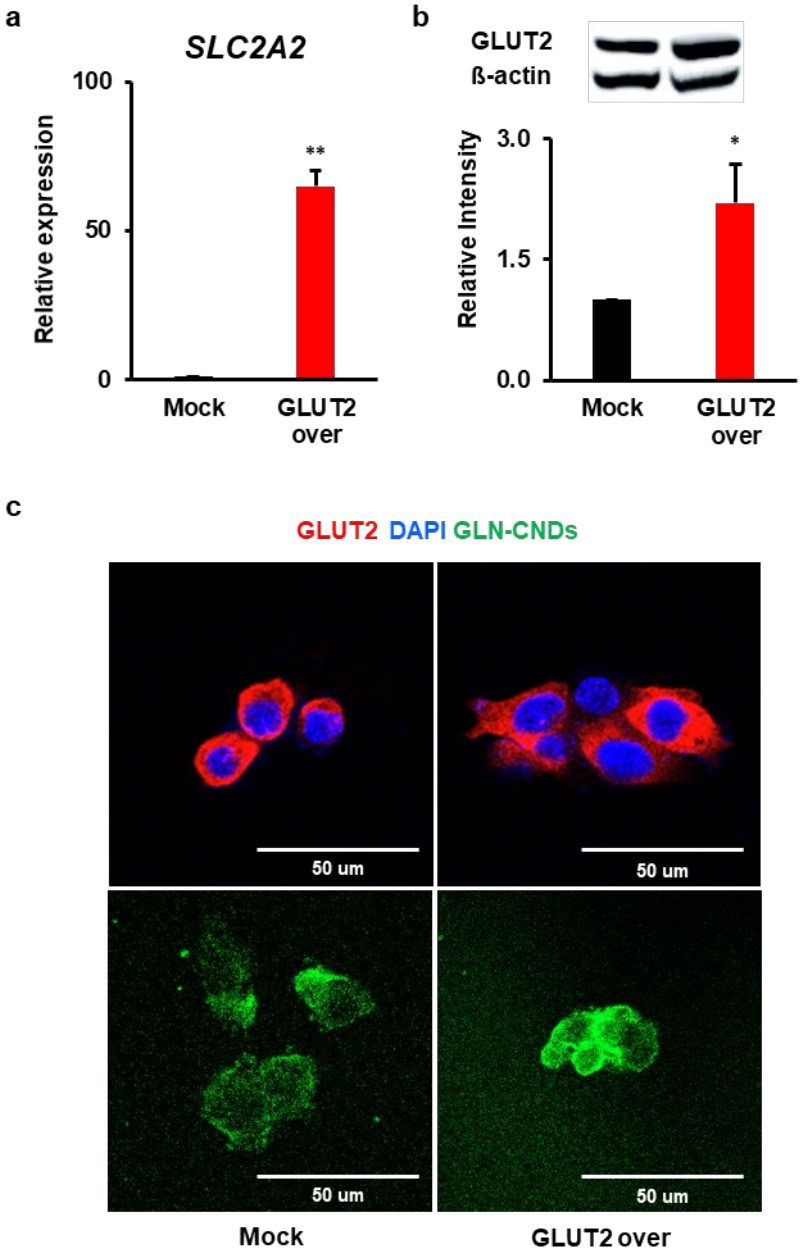

Figure S18. GLUT2 was upregulated in HepG2 human HCC cells. (a) *SLC2A2* expression levels were determined using quantitative real-time polymerase chain reaction (qPCR) in GLUT2 overexpression cells compared with the control cells (n = 3). (b) Protein levels of GLUT2 were analyzed by western blotting (n = 5). (c) Cells were co-stained with the anti-GLUT2 antibody and DAPI or GLN-CNDs (n = 5). Images were obtained by confocal microscopy.

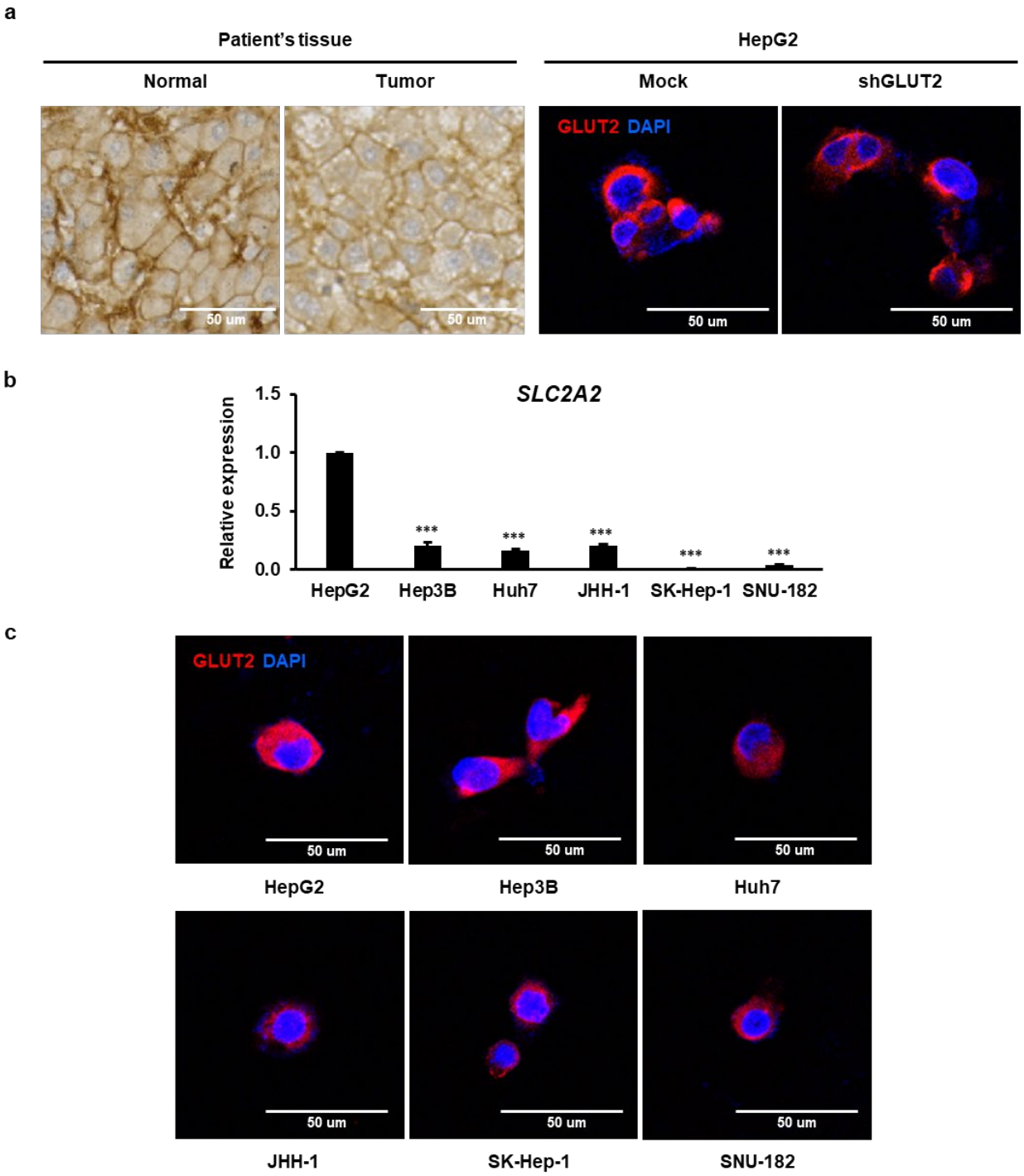

Figure S19. The subcellular distribution of GLUT2 in patient's tissues and HepG2 cells. (b) *SLC2A2* expression levels were determined using quantitative real-time polymerase chain reaction (qPCR) in human HCC cell lines (n = 4). (c) GLUT2 protein distribution was visualized by confocal microscopy in human HCC cell lines (n=5).

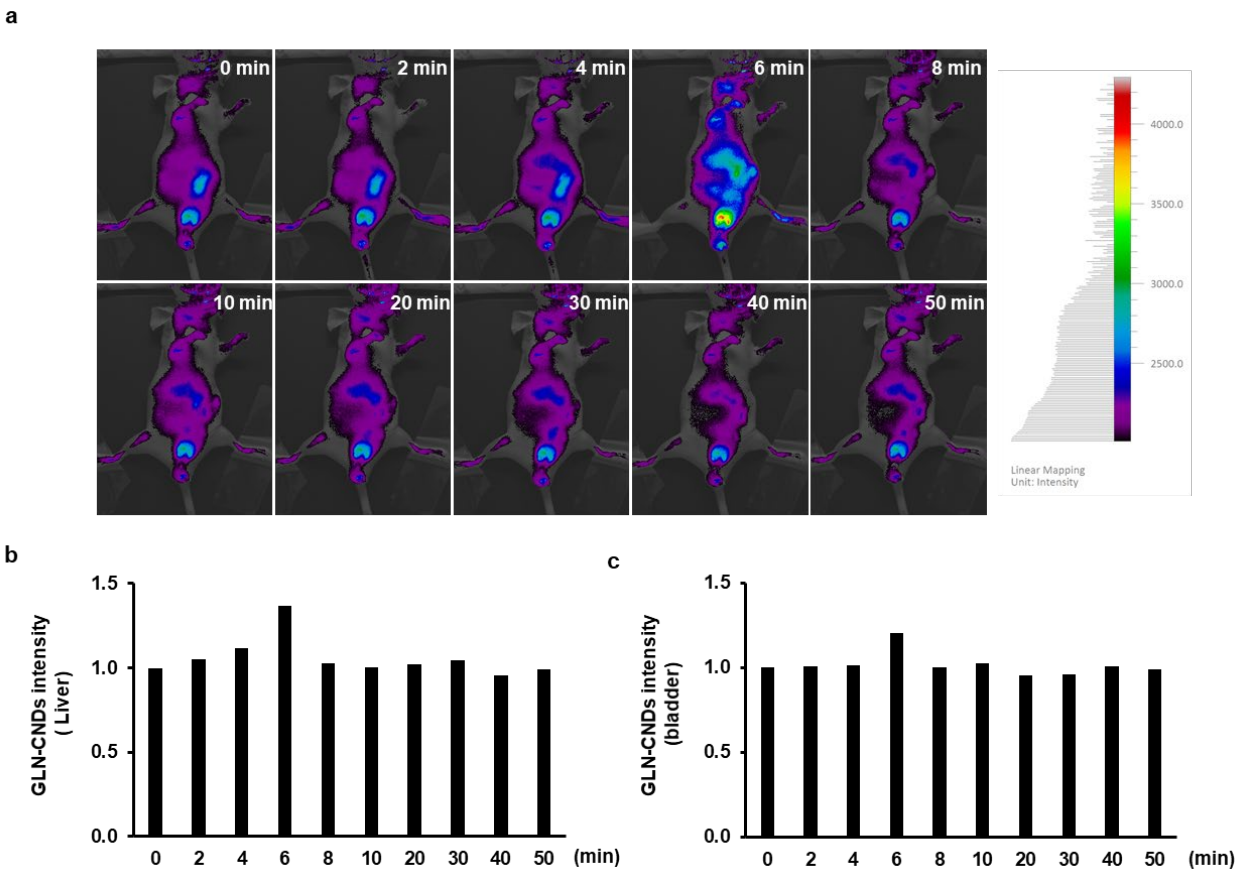

Figure S20. (a) The biodistribution of near-infrared GLN-CNDs. GLN-CND was observed by. intravenous injections into the lateral tail veins of nude mouse. (b, c) The near-infrared signal was measured in liver and bladder.